

Electrochemical Performance of MnO₂ Composite with Activated Carbon for Supercapacitor Applications

Sunaina Saini^{a*}, Prakash Chand^a, & Aman Joshi^{a,b}

^aDepartment of Physics, National Institute of Technology, Kurukshetra 136 119 India

^bDepartment of Physics, J C Bose University of Science and Technology, YMCA Faridabad, 121 006, India

Received: 10 May 2023; Accepted: 30 May 2023

Electric vehicles/hybrid electric vehicles, next-generation personal electronics, and stationary storage have all benefited from the energy storage system (ESS) revolution. The preparation of new and especially eco-friendly electrode material is an important task in the development of modern electrochemical energy storage devices. In the present work, MnO₂ nanostructures in composite with activated carbon were synthesized via a facile hydrothermal method. X-ray Diffraction (XRD) and a Scanning Electron Microscope (SEM) were used to examine the structure, crystallite size, and morphology of the produced samples (SEM). The absence of an impurity peak in the X-ray diffraction pattern suggested that MnO₂ nanostructures formed in the tetragonal phase. The Scherrer formula was used to determine the typical size of the crystallites. The creation of nanosheets and nanorods, as seen by SEM analysis, also contributed to the improved charge storage capacity. Also, the electrochemical properties of synthesized material were studied through a three-electrode system by using KNO₃ and KOH as aqueous electrolytes. The Cyclic Voltammetry (CV) and the Galvanostatic Charge-Discharge (GCD) study showed that the KNO₃ electrolyte is more suitable as the capacitance obtained is much higher in comparison with KOH. The highest specific capacitance of 317 F/g is achieved at 1A/g current density for the KNO₃ electrolyte. Furthermore, Electrochemical Impedance Spectroscopy (EIS) confirmed that the resistance offered by KOH is higher for this composite. The research found that the synthesized material might be employed for supercapacitor applications as their electrode material.

Keywords: Manganese Oxide, Activated Carbon, Morphology, Composite; Electrolyte, Supercapacitors

1 Introduction

The recent energy crisis brought on by rising resource demands and growing fossil fuel usage has encouraged people to constantly research renewable energy sources and new sorts of energy storage technologies¹. Some examples of energy storage technologies are batteries, fuel cells, capacitors, and supercapacitors. Due to high power density, fast response, and long life span, supercapacitors (SCs) are emerging as promising energy storage devices². They are categorized into three types such as EDLCs (Electric double-layer capacitors), PCs (Pseudocapacitors), and hybrid capacitors. Due to their eco-friendliness, excellent storage capacity, quick charge-discharge, and high specific capacitance, supercapacitors have numerous applications in industrial fields, the majority of which are for the automotive industry and military purposes³. The mechanisms for storing charge in both types of supercapacitors, i.e., in electric double-layer capacitors and pseudocapacitors, are different⁴. Pseudocapacitors store energy

electrochemically through quick surface-controlled redox processes, in contrast to electric double-layer capacitors, where charge storage is accomplished via the deposition of ions onto the electrode surface, i.e., electrostatically⁵. The electrochemical characteristics of pseudocapacitors are quite similar to that of double-layer capacitors, but the mechanism of storing charge is different; therefore prefix "pseudo" is used⁶. Pseudocapacitors provide a method for generating both high energy and high power densities because they quickly and reversibly conduct surface-controlled faradic reactions at the electrode surface by either insertion or deposition of electrolytic ions⁷. The materials required for pseudocapacitors include transition metal oxides such as Co₂O₃, RuO₂, WO₃, MnO₂, NiO, SnO₂, and conducting polymers like polypyrrole, polyaniline (PANI) etc⁸. Transition metal oxides are attractive as electrode materials for energy storage applications due to their enormous reserves, higher specific capacitance and different morphologies obtained during synthesis⁹. RuO₂ and MnO₂ are the most studied transition metal oxides as their theoretical

*Corresponding authors (Email: sunaina.inias@gmail.com)

specific capacitance is high with a better life span and good rate capability, but high price and toxicity have prevented RuO_2 from being widely used¹⁰. In contrast, MnO_2 is both inexpensive and eco-friendly because of its lack of toxicity and widespread availability¹¹. Ming and companions electrodeposited MnO_2 on the nickel substrate with different voltages and discovered that a maximum capacitance of 469 F/g is obtained when the deposition potential is 0.6 V with 83.9% retention after 2500 cycles¹². Wu *et al.* prepared MnO_2 nanostructures supported by nickel foam with 3D plate-like morphology and achieved nearly 680.6 F/g specific capacitance with 100% retention after 4000 cycles¹³. To improve the conductivity and cycle stability of different metal oxides, composite materials are created. Graphene, carbon nanotubes (CNTs), carbon aerogel, and activated carbon are all extensively utilized components in carbon nanocomposites because they have a large surface area and conductivity. Rao and colleagues developed α - MnO_2 using the coprecipitation method on carbon nanofibres (CNF), and they investigated that α - MnO_2 had the maximum capacitance of 313 F/g at 1A/g when CNF wt% is 1.25¹⁴. By using the template method, Xie and associates created porous MnO_2 and attained the high specific capacitance in 1M Na_2SO_4 of about 218 F/g at 0.1 A/g¹⁵. Fan *et. al* prepared the MnO_2 -CNT composite by ultrasonically mixing the as-prepared MnO_2 powder with the CNT in different weight ratios and the composite with 20% wt ratio exhibited better electrochemical behaviour *i.e.* 238.7 F/g in comparison with the pristine MnO_2 which could reach only 78.6 F/g capacitance¹⁶. Exfoliation of graphite produces graphene, a 2D planar structure comprising of carbon atoms in single layer¹⁷. Because of its exceptional conductivity (106 S m^{-1}) and large surface area (2630 m^2), it possesses a high theoretical capacitance of 550 F/g¹⁸. It also has high electrical conductivity ($200,000 \text{ cm}^2 \text{ V}^{-1} \text{ s}^{-1}$) and tremendous mechanical strength, making it an excellent material for the applications of energy storage¹⁹. Restacking graphene nanolayers, which causes loss in surface area due to close interlayer spacing, is the primary obstacle to its use in practical applications. As a result, most researchers choose to incorporate MnO_2 between the layers for developing MnO_2 /Graphene composites in order to minimise graphene aggregation²⁰. Argüello *et. al* synthesized the manganese oxide composite with graphene nanoplatelets via Electrophoretic Deposition method (EPD) and achieved the high specific capacitance of 224 F/g in basic electrolyte²¹. So, in this direction, we also prepared the MnO_2 composite with

activated carbon using the hydrothermal method and investigated the electrochemical performance in two different electrolytes *i.e.*, neutral and basic electrolytes. The role of electrolytes is essential while interacting with electrode material during the electrochemical reactions so that the best electrolyte can be chosen for high-performance super capacitors. Although the potential window is large for organic electrolytes, we preferred here only aqueous electrolytes because they have high conductivity and also the capacitance retention is maintained for large number of charge-discharge cycles in comparison with organic electrolytes. We obtained high specific capacitance value in 1M KNO_3 electrolyte *i.e.* 317 F/g at 1 A/g current density. Therefore, we can consider that MnO_2 nanoparticles in composite with activated carbon as an excellent choice for use in supercapacitor applications on the basis of their electrochemical properties

2 Materials and Methods

2.1 Procedure to synthesize α - MnO_2 composite with activated carbon

The reagents used in the complete synthesis process are Potassium Hydroxide pellets [$>99\%$ purity, Loba Chemie] and Hydrochloric acid [37% (w/w), Loba Chemie]. Carbon black, N-Methyl-2-pyrrolidone (NMP), and Polyvinylidene fluoride (PVDF) are purchased from Sigma-Aldrich for the fabrication of electrodes. Activated carbon, Manganous sulfate monohydrate, and Potassium permanganate were purchased from Fisher Scientific Pvt. Ltd. with 99% purity. According to the synthesis process of α - MnO_2 composite with activated carbon depicted in Fig. 1, the manganous sulfate is first dissolved in deionized water.

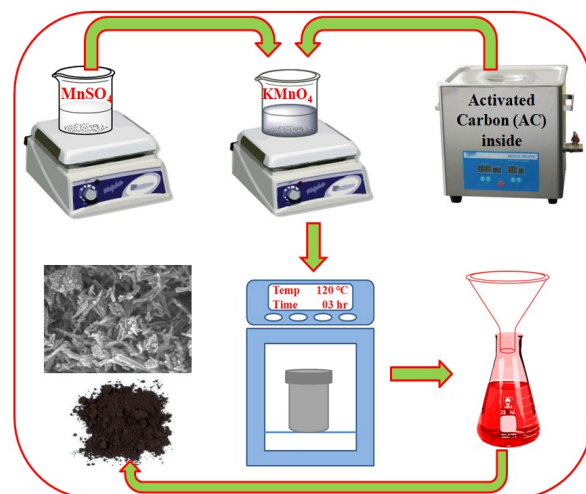
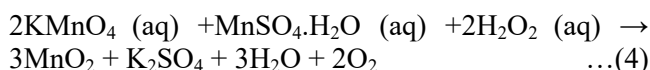
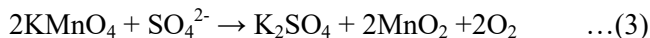
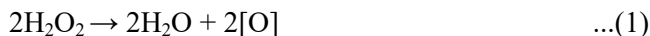


Fig. 1 — Synthesis of α - MnO_2 composite with activated carbon.

The activated carbon was ultrasonically treated for 30 minutes so that the stacking of layers could be removed, and added this solution to the Manganous sulfate solution. In deionized water that has a trace amount of hydrogen peroxide added to it, the stoichiometric ratio of potassium permanganate is dissolved. Now, the solution that was previously prepared is added drop by drop into the solution that already contained KMnO_4 and H_2O_2 , which results in the formation of the brown-colored solution. The 100 ml Teflon container is then filled to between 70-80 percent of the top with this solution. In order to reach the desired level of pressure within the Teflon bottle, the bottle is then placed into the hydrothermal setup made of stainless steel, and the lid is screwed on as firmly as possible. For the completion of the reaction necessary to produce manganese oxide, this apparatus is placed inside an oven and subjected to temperatures of 150°C for a period of three hours. After bringing the temperature down to room temperature, the precipitates, blackish-brown in color, are collected and washed with DI water and ethanol to remove any precursor ions. The precipitates are then dried for 4-5 hours at 80°C to complete the process. The reactions that take place during the formation of the $\alpha\text{-MnO}_2$ composite are broken down and illustrated below.



Therefore, hydrogen peroxide is utilized in this process for the production of manganese oxide, which reduces the manganese precursors for the easy flow of electrons.

2.2 Characterizations and Electrode Fabrication

The microstructure of the prepared MnO_2 composite was confirmed using X-ray Diffraction characterization (XRD; Rigaku Japan). The X-rays emitted from the $\text{Cu-K}\alpha$ radiation source ($\lambda = 0.15405 \text{ nm}$) were scanned at the rate of $2^\circ/\text{minute}$ within the range 10° to 80° . The morphological investigation for the sample was done by utilizing Field Emission Scanning Electron Microscopy (FESEM; JEOL 7610F Plus). The three-electrode configuration that utilizes the aqueous electrolyte (KOH and KNO_3) consists of a working electrode composed of MnO_2 composite with activated carbon, silver/silver

chloride as the reference electrode, and a platinum wire as the counter electrode. This three-electrode system is typically used to detect the potential difference between the working and reference electrodes without actually passing a current through the device. To this end, characterizations such as CV, GCD, and EIS were performed subsequent to electrode manufacturing. The electrodes are manufactured by grinding together 10% weight of Polyvinylidene (PVDF), 10% weight of carbon black and 80% weight of synthesized carbon materials to create a homogenous mixture. Several droplets of an organic solvent (N-methyl-2-pyrrolidone) dissolved the above-mentioned combination. The mass of the electrode was measured before and after they were coated with the active material and found to be nearly 1 mg. These electrodes of MnO_2 composite with activated carbon were electrochemically characterized by employing CHI 760E Electrochemical instrument with the techniques like CV (Cyclic Voltammetry), GCD (Galvanostatic Charging-Discharging), and EIS (Electrochemical Impedance Spectroscopy).

3 Results and Discussions

3.1 Structural and Morphological Analysis

The XRD spectrum shown in Fig. 2 is analyzed to validate the crystal structure of the prepared composite material. The characteristic peak confirms the creation of a tetragonal phase of $\alpha\text{-MnO}_2$ nanoparticles, which coincided with the standard accessible JCPDS data #440141²². The sharp and intense peak that appears at about 37.6° belongs to the (211) plane. The sample not exhibited any impurity peak in its XRD spectrum, so it can be concluded that the materials that were synthesized are of very high purity. In the present case, the incorporation of

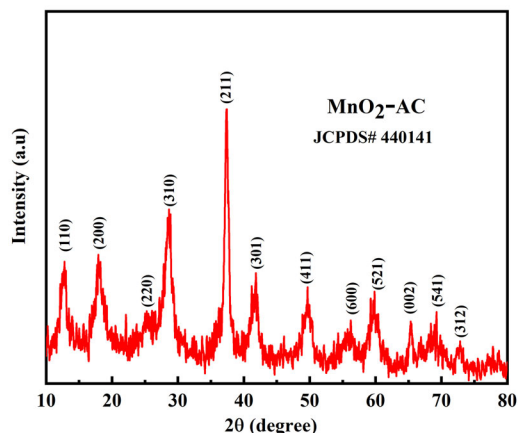


Fig. 2 — XRD spectra of $\alpha\text{-MnO}_2$ -activated carbon composite.

activated carbon resulted in the broadening of the peaks, as well as a small shift in angle, indicating a low crystallinity structure. The obtained samples have a slight variation in their lattice parameters that can be estimated using the equation given below.

$$\frac{1}{d^2} = \frac{h^2+k^2}{a^2} + \frac{l^2}{c^2} \quad \dots(5)$$

$2d \sin\theta = n\lambda$ is the formula used to estimate the interplanar distance denoted by 'd'. The particular value of 'd' and ' θ ' satisfies Bragg's law. We obtain the peak of the diffraction pattern that is associated with that specific plane having miller indices h, k and l. The Debye-Scherrer equation is a widely used method to determine the typical crystallite size.

$$D = \frac{0.9\lambda}{\beta \cos\theta} \quad \dots(6)$$

Equation 6 illustrates how the Full-Width Half Maxima (β) of the peaks in the XRD spectrum may be utilized to calculate the average crystallite size where θ is the Bragg angle and λ is the wavelength. The low-intensity peaks obtained for this composite material also indicate that its crystallite size is smaller.

Figures 3(a–d) displays the FESEM images of prepared composite material with a scale of 100 nm. The micrographs revealed the morphology of the samples by generating the signals through electron interaction with the sample and obtained information about the surface composition and topography. The mixed morphology is evident that the small rods belong to magnesium oxide, and the platelets indicate the presence of activated carbon. Due to this mixed morphology, the surface area of the nanoparticles increases, which in turn boosts the material's electrochemical performance by decreasing the path of electrons to travel and the time it takes for electrolytic ions to diffuse. Nanorods, due to their homogeneity, make ion transfer much simpler than it already is by reducing the particle size to a negligible value.

3.2 Electrochemical Study

To determine the kind of charge storage processes occurring in the electrode material, CV is one of the important techniques based on continuously varying potential differences with a constant scan rate. When the electric potential reaches either its lowest or its

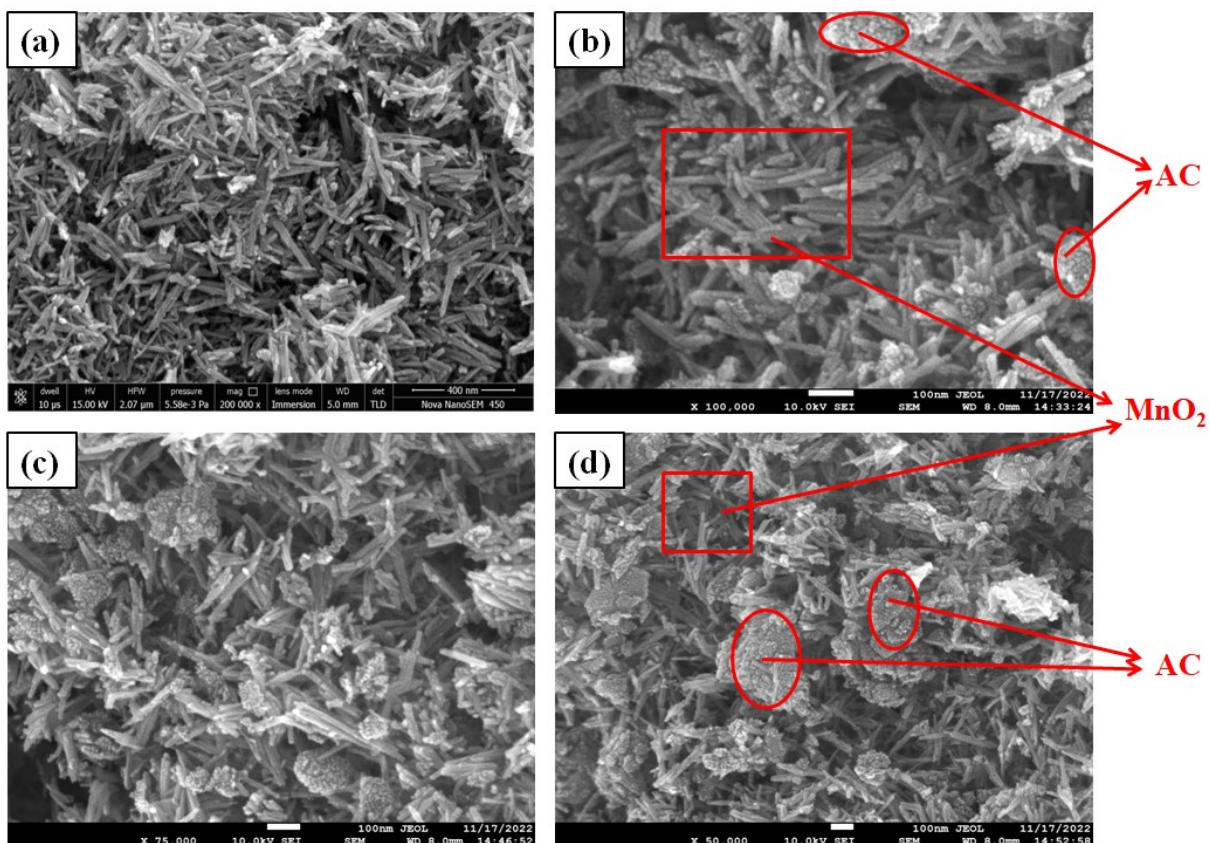


Fig. 3 — (a-d) FESEM images of α - MnO_2 -activated carbon composite.

maximum value, the scan rate is inverted, and the current intensity is evaluated in relation to the electric potential. The shape of the CV curves exhibits the type of behavior (capacitive/diffusive) taking place at the junction of the electrode and electrolyte. In the present study, CV curves depicted in Figs. 4 (a-b) displayed different behavior in both electrolytes because of the intercalation process along with the EDLC behavior due to surface storage.

$$C = \frac{\int Idv}{2m \times \Delta v \times V} \quad (7)$$

Where ' Δv ' is the potential window, ' V ' is the scan rate (mVs^{-1}), $\int Idv$ is the area enclosed by the loop, ' m ' is the mass difference before and after loading the material (mg). From the shape of CV loops, It was discovered that the CV curves resemble intercalation pseudo capacitance behavior due to the occurrence of redox peaks in the basic electrolyte (KOH), but for neutral electrolyte (KNO_3), a somewhat rectangular shape is obtained for CV curves. In the case of basic electrolytes, the diffusion-controlled mechanism is mainly accountable as there are distinct oxidation reduction peaks clearly visible, but for neutral

electrolytes, there is the creation of a double layer through absorption which is the primary source of the capacitive contribution. The potential window of the sample lies between -0.2V to 0.8V for the KNO_3 electrolyte, while in the case of the KOH electrolyte, it ranges from -4V to 4V . The effect of the electrolyte changed the potential window as well as the specific capacitance by varying the charge storage mechanism. The area under the curves keeps increasing as the sweep rate changes from 6 to 20 mV/s without distorting the shape of the curve, which further demonstrates the material's stability. The specific capacitance will decrease in proportion to the increase in the scan rate, which is also made clear from the estimation of CV curves. This is due to the fact that most of the time, fast reversible reactions will occur when the scan rate is high, and the ions will not have adequate time to penetrate deep within the matrix. As a result, all of the electroactive sites will be inaccessible. Figures 5 (a, b) exhibits the GCD curves of nanocomposite in neutral and basic electrolytes with current density ranging from 1 Ag^{-1} to 5 Ag^{-1} . The constant current intensity is applied in galvanostatic charging-discharging studies. The amount of potential

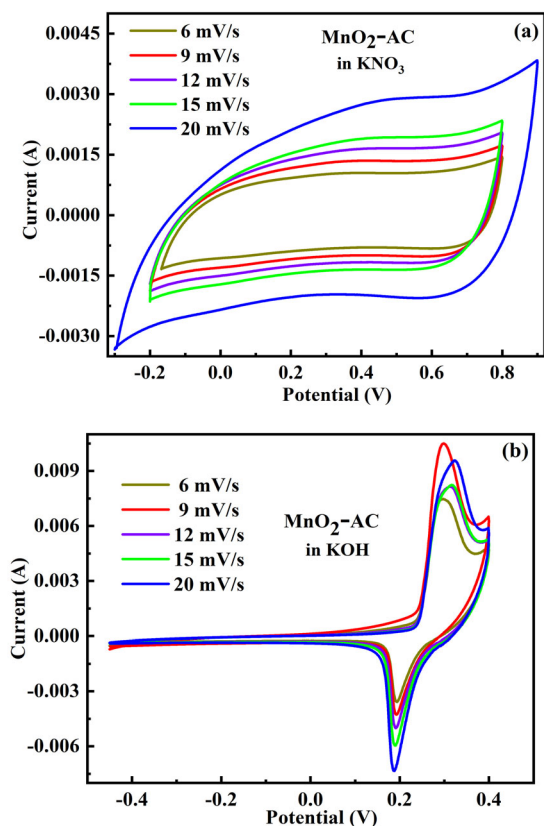


Fig. 4 — CV curves of composite (a) KNO_3 , and (b) KOH.

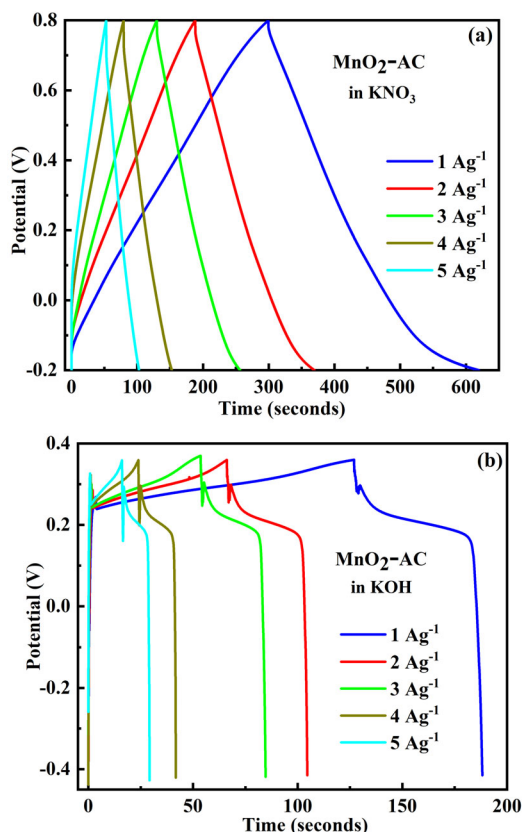


Fig. 5 — GCD curves of composite (a) KNO_3 , and (b) KOH.

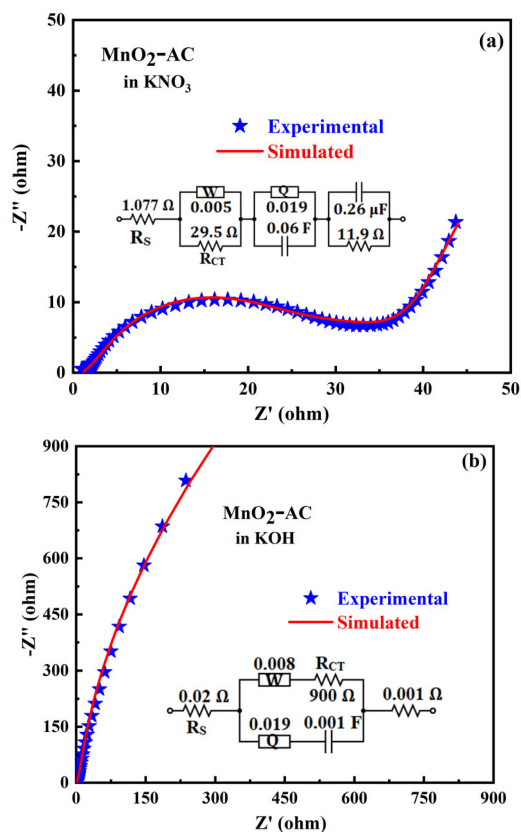
Table 1 — Value of Specific Capacitance for α -MnO₂-activated carbon composite in different electrolytes

Current density (Ag ⁻¹)	Specific capacitance (F/g)	
	KNO ₃	KOH
1	317	77.5
2	310	75
3	303	67.5
4	292	60
5	260	56.2

that can be recorded is going to be determined by the total charge that has been moved throughout the system. As the highest or lowest possible potential difference has been reached in this experiment, the present current intensity is reversed in polarity. GCD was performed at different current rates by using KNO₃ as a neutral electrolyte and KOH as a basic electrolyte. The pseudocapacitive nature is confirmed by the Quasi triangular shapes of the curves in the KNO₃ electrolyte. The comparison of the value of specific capacitance obtained for both the electrolytes at various current densities is encapsulated in Table 1 and calculated using the following equation.

$$C_{sc} = \frac{I \times \Delta t}{M \times \Delta V} \quad (\text{in F/g}) \quad \dots(8)$$

Where, I= Current applied, M= deposited mass on the substrate, ΔT = Time of discharging. In neutral electrolytes, because of the charge storage at the surface of the electrode material, the GCD curves demonstrate that the process of charging-discharging is nearly linear. On the other hand, in the case of a basic medium, the process of charging-discharging is non-linear due to the transition between Mn⁴⁺ \leftrightarrow Mn³⁺ ions at the time of reduction and oxidation. The charge can be stored in manganese oxide in one of two primary ways: either by simply storing the electrolytic ions at the junction of the material or by inserting ions into the voids of the material. The value of specific capacitance directly depends upon the discharging time, which drops as the current density is increased during GCD measurements. When the current density is low, the specific capacitance is high because the electrolytic ions have a greater amount of time to move throughout the material and accumulate sufficient charge there. However, there are diffusion restrictions inside the electrode material when the sweep rate of the current is increased, which does not allow the ions to access all available sites in a short duration of time, leading to a lower value of specific capacitance⁴. The high surface area affiliated with the mixed morphology offered by nanorods and

Fig. 6 — Nyquist plot of composite (a) KNO₃, and (b) KOH.

nanoplatelets accounts for this composite material's improved charge-storing capacity, allowing the ions to insert easily inside the material. Since most of the charge is kept exclusively at the surface, the rate capability of a neutral electrolyte remains better even at a high current density due to the increased surface area.

The electrochemical impedance spectroscopy (EIS) is analyzed in both electrolytes for MnO₂ composite electrodes to study the capacitive behavior and charge transfer mechanisms. This study may be performed at a number of other frequency ranges; however, the range from 0.1 Hz to 10⁵ Hz was found to be the most effective for analyzing all of the samples that were prepared for this research work. EIS is used to investigate the impedance of the material, and the results of this investigation are shown as a Nyquist plot with different shapes, as illustrated in Figures 6 (a-b). These shapes are determined by the specific characteristics of the sample. This plot may be characterized by utilizing a variety of capacitive and non-capacitive components, such as the Warburg resistance and the constant phase element. The non-ideal capacitive resistance is responsible for the generation of this constant phase

element Q^{23} . The semi-infinite linear diffusion process, which the Warburg resistance represents, predominates in low-frequency areas, while its value is negligible in high-frequency regions²⁴. At high frequencies, the diffusion-limited mechanism for electron mobility corresponds to the semicircle area of the Nyquist plot. The electron-transport resistance (R_{CT}) may be calculated by measuring its diameter. The other section, which is the linear portion of the Nyquist plot in the low-frequency domain, provides information about the diffusion process in the aqueous electrolytic solution. In this second part, we use individual or combined Nyquist components to analyze the electrochemical response of the manufactured electrodes in more detail²⁵. Electrode and electrolyte charge transfer cause the equivalent series resistance (R_s) which is displayed before the beginning of the semicircle in the Nyquist plot. The impedance study and simulated circuits revealed that the charge transfer resistance obtained in the neutral electrolyte is very low when compared with the basic electrolyte due to different charge storage mechanisms taking place in both cases. The charge storage is mainly pseudocapacitive in nature for KNO_3 , while the basic electrolyte resulted in a diffusion-controlled process.

4 Conclusion

We conclude that the MnO_2 -activated carbon composite is successfully synthesized using a simple hydrothermal process, and its structural, morphological, and electrochemical properties can be examined. X-ray diffraction (XRD) analysis confirmed the sample's crystal structure and determined its phase. FESEM analysis exhibited that the mixed morphology is obtained in which small rods belong to magnesium oxide and the platelets indicate the presence of carbon, and a larger surface area maximizes the charge-storing capacity. The electrolyte also played a vital role in optimizing the specific capacitance of the sample prepared for electrodes, as evidenced by the fact that the highest capacitance is obtained for the neutral electrolyte in both the CV and GCD analyses. Nyquist plot circuit diagrams simulated by both electrolytes show the varying resistances of the constituent parts. Because of its favorable electrochemical behavior, the MnO_2 -activated carbon composite is a promising candidate for use in supercapacitor devices.

Acknowledgment

One of the authors, Sunaina Saini, is thankful to the Director of NIT Kurukshetra for providing the Institute

fellowship and Sophisticated laboratories in the Physics Department. Author Prakash Chand is grateful to SERB, DST Project for affording the CHI 760E Instrument with grant number SERB/F/ 10804/2017-18.

References

- Liu H, Xu T, Liu K, Zhang M, Liu W, Li H, Du H, & Si C, *Ind Crops Prod*,165 (2021) 113425.
- Liu S, Wei L, & Wang H, *Appl Energy*,278 (2020) 115436.
- Najib S & Erdem E, *Nanoscale Adv*,1(2019) 2817.
- Saini S & Chand P, *Chem Phys Lett*,802 (2022) 139760.
- Saini S, Chand P & Joshi A, *J Energy Storage*,39 (2021) 102646.
- Chodankar N R, Pham H D, Nanjundan A K, Fernando J F S, Jayaramulu K, Golberg D, Han Y & Dubal D P, *Small*,16 (2020) 2002806.
- Augustyn V, Come J, Lowe M A, Kim J W, Taberna P L, Tolbert S H, Abruña H D, Simon P, and Dunn B, *Nat Mater*, 12 (2013) 518.
- González A, Goikolea E, Barrena J A & R Mysyk, *Renew Sustain Energy Rev*,58 (2016) 1189.
- An C, Zhang Y, Guo H, & Wang Y, *Nanoscale Adv*1(2019) 4644.
- Zhang Y & Xue D, *Mater Focus*,2 (2013)161.
- Johnson C S, *J Power Sources*,165 (2007) 559.
- Zhang M, Chen Y, Yang D, & Li J, *J Energy Storage*,29 (2020) 101363.
- Wu C, Zhu Y, Ding M, Jia C & Zhang K, *Electrochim Acta*,291 (2018) 249.
- Rao T P, Kumar A, Naik V M & Naik R, *J Alloys Compd*,789 (2019) 518.
- Xie X, Zhang C, Wu M B, Tao Y, Lv & Yang Q H, *Chem Commun*49 (2013) 11092.
- Fan J, Chen Z, Tang N, Li H & Yin Y, *IEEE Int Conf Nanotechnol*, (2013) 933.
- Hernandez Y, Nicolosi V, Lotya M, Blighe F M, Sun Z, De S, McGovern I T, Holland B, Byrne M, Gun'Ko Y K, Boland J J, Niraj P, Duesberg G, Krishnamurthy S, Goodhue R, Hutchison J, Scardaci V, Ferrari A C & Coleman J N, *Nat Nanotechnol*,3 (2008) 563.
- El-Kady M F, Strong V, Dubin S & Kaner R B, *Science*, 335 (2012) 1326.
- Bolotin K I, Sikes K J, Jiang Z, Klima M, Fudenberg G, Hone J, Kim P & Stormer H L, *Solid State Commun*,146 (2008) 351.
- Sheng L, Jiang L, Wei T & Fan Z, *Small*, 12 (2016) 5217.
- Argüello J A, Cerpa A & Moreno R, *Ceram. Int*.45 (2019) 14316.
- Sunaina, Chand P, Joshi A, Lal S & Singh V, *Chem. Phys Lett*777 (2021) 138742.
- Bard A J & Faulkner L R, *Electrochemical Methods Fundamentals and Applications*,(Wiley, 1980).
- Nithya V D, Hanitha B, Surendran S, Kalpana D & Selvan R K, *Ultrason. Sonochem*,22 (2015) 300.
- Mayorga-Martinez C C, Cadevall M, Guix M, Ros J & Merkoçi A, *Biosens. Bioelectron*,40 (2013) 57.